Uplink Cell Capacity of Cognitive Radio Networks with Peak Interference Power Constraints

Xuemin Hong[†], Cheng-Xiang Wang[†], and John Thompson[††]
[†]Joint Research Institute for Signal and Image Processing, Heriot-Watt University, Edinburgh, EH14 4AS, UK.
[††]Joint Research Institute for Signal and Image Processing, University of Edinburgh, Edinburgh, EH9 3JL, UK.
Email: xh12@hw.ac.uk, cheng-xiang.wang@hw.ac.uk, john.thompson@ed.ac.uk

***Abstract*—A cognitive radio (secondary) network can reuse the under-utilized spectrum licensed to a primary network on a non-interruptive basis. In this paper, we study the uplink capacity of a secondary network where a secondary base station (BS) is located at the center while multiple secondary users are uniformly distributed within a circular cell of radius R. Primary users are assumed to be distributed in the same plane according to a Poisson point process with a density parameter λ_p. To protect primary services, secondary users can only transmit under a peak interference power constraint which guarantees that the instantaneous interference power perceived by any primary user is not larger than a certain threshold. In addition, we assume an opportunistic scheduler at the BS which exploits multi-user diversity among M secondary users and stochastically maximize the cell capacity. We first study the capacity with a simple channel model considering only the path loss and derive the closed-form cumulative distribution function (CDF) of the capacity. We then study the capacity with realistic fading channel models using a semi-analytical approach. The impacts of the parameters R, λ_p, and M on the capacity are quantified and discussed. Moreover, we find that shadowing and fading only have limited impacts on the distribution of the capacity.**

I. Introduction

The radio spectrum is a precious natural resource that underpins various wireless services. The spectrum is traditionally regulated by a fixed frequency assignment policy which assigns frequency bands to license holders for exclusive use. Such a static spectrum licensing policy eliminates interferences among different radio systems in a brutal-force way but results in very inefficient spectrum utilization [1]. Dynamic spectrum access (DSA) has been proposed as a promising approach to improve the spectrum utilization by allowing new wireless systems to dynamically access/share the licensed band on a negotiated or an opportunistic basis [2].

DSA strategies can be broadly categorized into three models [2]: dynamic exclusive use model, open sharing model, and hierarchical access model. The first model maintains a rigid license-based policy but introduces more flexibility to allow license holders to lease or trade their spectrum freely by means of spectrum property rights or dynamic spectrum allocation. The open sharing model embraces an unlicensed philosophy and allows peer users to have equal spectrum access rights and utilize a common spectrum locally without interfering with each other. The last model adopts a hierarchical access structure with primary and secondary users. It allows the secondary users to access the licensed spectrum under the condition that no harmful interference is caused to the primary users (licensees). To achieve this, it is usually a requirement for secondary users to be aware of the radio environment and dynamically adjust their transceiver parameters. Therefore, "secondary network" is also often referred to as "cognitive radio network" in the literature [3], [4]. In this paper, we restrict our study on cognitive radio networks in the hierarchical access model.

The coexistence of primary and secondary networks is a two-fold problem. First of all, the quality-of-service (QoS) of the primary network should not be (significantly) degraded due to the presence of the secondary network. Technically, this can be achieved by controlling the interference power perceived at primary receivers to fulfill certain constraints such as peak interference power constraint [6], [7], average interference power constraint [6], [7], or interference outage constraint [8]. To this end, several interference models have been proposed in [9]–[11] to provide metrics of measuring such interferences.

On the other hand, a secondary network needs to provide a reasonable capacity to justify its deployment cost. Unlike conventional licensed networks, the capacity of a secondary network is significantly affected by the coexisting primary system [12]. Such a capacity is first bounded by the interference constraint which in turn limits emission powers of secondary transmitters. Moreover, interferences generated by the primary network will further degrade the secondary network capacity. The information-theoretic capacity of a secondary/cognitive radio link has been analyzed in [13] in Gaussian channels. In [6], [7], the capacities have been investigated in fading channels under peak or average interference power constraints. These analyses [6], [7], [13], however, are restricted to the capacity of a single link without taking into account the effects of user distribution and path loss. In our previous work [14], [15], we have extended the capacity analysis to the network level under average interference power constraints. In this paper, we focus on the capacity of a secondary network under peak interference power constraints.

The remainder of this paper is organized as follows. Section II describes the system model. In Sections III and IV, we study the capacity of the secondary network with simple channel models and realistic channel models, respectively. Numerical results and discussions are presented in Section V. Finally, conclusions are drawn in Section VI.

978-1-4244-2063-4/08/$25.00 ©2008 IEEE

II. System Model

The system model is shown in Fig. 1 where primary users (TV receivers) and secondary users (mobile phones) coexist on a plane. The primary users are denoted as V_i $(1 \leq i < \infty)$ and their distribution follows a Poisson point process with a density parameter λ_p, which denotes the average number of primary users per unit area. We consider a secondary circular cell with a BS located at the center and M secondary users, denoted as U_j $(1 \leq j \leq M)$, uniformly distributed within the cell. The cell radius is denoted as R. In this paper, we focus on the uplink capacity analysis of the secondary cell, while the same approach can be easily extended for downlink analysis.

We assume that multiple secondary users transmit in orthogonal channels to avoid mutual interferences. In this paper, we use a time division multiple access (TDMA) scheme, which implies that at any time slot, the target secondary user is the only interference source to the primary network. We refer the underlying channels from secondary transmitters to primary receivers as *interference channels*. The instantaneous channel power gains from the jth secondary user to the ith primary receiver is denoted as $h^I_{i,j}$. The jth secondary user, once scheduled to transmit, should control its transmission power P_j so that the interference power perceived at primary receivers $I_i = P_j h^I_{i,j}$ fulfill certain constraints. In this paper, we consider a peak interference power constraint given by $I_i \leq I_0$, where I_0 is the maximum interference power that a primary receiver can tolerate. If we further denote

$$h_j^{I_{\max}} = \max_i (h^I_{i,j}) \tag{1}$$

as the largest interference channel gain associated with the jth secondary user, it follows that the maximum allowable transmit power of the jth secondary user is given by

$$P_j^{\max} = I_0 / h_j^{I_{\max}}. \tag{2}$$

In practice, a secondary transmitter may obtain the information of $h_j^{I_{\max}}$ by means of common control channels [16] or primary receiver detection [17].

On the other hand, we refer the underlying channels from secondary transmitters to the center BS as *access channels*. The instantaneous channel power gain from the jth secondary user to the BS is denoted as h^A_j. We assume that the channel state information $\{h^A_j\}$ and $\{h_j^{I_{\max}}\}$ is known to the BS by means of channel estimation and feedback from secondary users. The BS can then estimate the potential received power given by the jth secondary user as

$$S_j = P_j^{\max} h^A_j = I_0 h^A_j / h_j^{I_{\max}}. \tag{3}$$

The values of S_j vary among different secondary users. Therefore, the BS can exploit this multi-user diversity by allocating the next available time slot to the secondary user with the largest S_j. This is also known as opportunistic scheduling which can maximize the cell capacity. With a perfect opportunistic scheduler, the signal power received at the BS is given by

$$S = \max_j (S_j) \quad (1 \leq j \leq M). \tag{4}$$

It follows that the instantaneous uplink capacity perceived at the BS, normalized over the bandwidth, is given by

$$C = \log_2(1 + S/\Omega) \tag{5}$$

where Ω denotes the total interference and noise power received at the BS. Clearly, the uplink capacity C is a random variable, whose distribution will be analyzed subsequently.

III. Capacity under Simple Channel Models

Simple channel models that only consider the effect of pathloss regardless of random shadowing and fading have been adopted in some cognitive radio network studies [12], [14], [15]. The reason of using simple channel models is that they often lead to elegant analytical results which can reveal important insights without over-complicating the problem. In this section, we adopt simple channel models and aim to find the closed-form CDF of the capacity C.

When only the pathloss is considered, we have

$$h^I_{i,j} = K^I / (d^I_{i,j})^\alpha \tag{6}$$

$$h^A_j = K^A / (d^A_j)^\alpha \tag{7}$$

where K^I and K^A are pathloss-related constants for the interference and access channels, respectively, $d^I_{i,j}$ is the distance between the ith primary receiver and the jth secondary transmitter, d^A_j is the distance between the jth secondary transmitter and the BS, and α is the pathloss exponent ranging from 2 to 5 [18]. Substituting (6) to (1), it follows that (2) can be rewritten as

$$P_j^{\max} = \frac{I_0}{K^I} \left(d_j^{I_{\min}} \right)^\alpha \tag{8}$$

where $d_j^{I_{\min}} = \min(d^I_{i,j})$ is the distance between the jth secondary transmitter to the nearest primary receiver. According to the properties of Poisson point processes [19], $(d_j^{I_{\min}})^2$ follows an exponential distribution given by

$$f_{(d_j^{I_{\min}})^2}(x) = \lambda_p \pi \exp\left(-\lambda_p \pi x\right). \tag{9}$$

From (8) and (9), the CDF of $P_j^{\max}$ can then be derived using the transformation of random variables [20] with the following expression

$$F_{P_j^{\max}}(x) = 1 - \exp\left(-\lambda_p \pi (x K^I / I_0)^{2/\alpha}\right). \tag{10}$$

Substituting (6) and (7) into (1) and (3), we have

$$S_j = I_0 \frac{K^A}{K^I} \left(\frac{d_j^{I_{\min}}}{d^A_j} \right)^\alpha. \tag{11}$$

Since the secondary users are uniformly distributed in the cell, $(d^A_j)^2$ follows a uniform distribution ranging from 0 to R^2. Using the transformation of random variables, it is easy to show that the CDF of S_j is given by

$$F_{S_j}(x) = 1 - \frac{1 - \exp(\lambda_p \pi R^2 (x/K)^{2/\alpha})}{\lambda_p \pi R^2 (x/K)^{2/\alpha}} \tag{12}$$

where K is a constant given by $K = I_0 K^A / K^I$. We assume that the received powers S_j from different secondary users are mutually independent and follow the same CDF given by (12). With opportunistic scheduling, the received signal power S has a CDF given by $F_S(x) = \left[F_{S_j}(x)\right]^M$. It follows that the CDF of the uplink capacity C can be obtained as

$$F_C(x) = F_S\left(\Omega(2^x - 1)\right) = \left[F_{S_j}\left(\Omega(2^x - 1)\right)\right]^M. \quad (13)$$

IV. Capacity under Realistic Channel Models

In this section, we adopt more realistic channel models considering not only the effects of pathloss but also shadowing and fading.

A. Realistic Channel Models

As modifications of the simple channel model in (6) and (7), the realistic channel models are given by

$$h_{i,j}^I = K^I \xi_{i,j}^I \eta_{i,j}^I / (d_{i,j}^I)^\alpha \quad (14)$$

$$h_j^A = K^A \xi_j^A \eta_j^A / (d_j^A)^\alpha \quad (15)$$

where $\xi_{i,j}^I$ and $\eta_{i,j}^I$ are random variables which model the effects of the shadowing and mutlipath fading in the interference channels, respectively. Similarly, ξ_j^A and η_j^A represent random shadowing and fading factors in the access channels, respectively. We assume that the shadowing factors $\{\xi_{i,j}^I\}$ and $\{\xi_j^A\}$ are mutually independent, each following a log-normal distribution with zero mean and a standard deviation σ_ξ ranging from 5 to 12 dB [18] with 8 dB being a typical value for macrocellular applications. We further assume that the fading factors $\{\eta_{i,j}^I\}$ and $\{\eta_j^A\}$ are also mutually independent and follow identical distributions $f_\eta(x)$. When Nakagami fading channels [18] are assumed, $f_\eta(x)$ is given by a Gamma distribution [18]

$$f_\eta(x) = \frac{m^m x^{m-1}}{\Gamma(m)} \exp(-mx), \quad m \geq \frac{1}{2} \quad (16)$$

where m is the Nakagami shape factor and $\Gamma(\cdot)$ denotes the gamma function.

The products $\{\xi_{i,j}^I \eta_{i,j}^I\}$ and $\{\xi_j^A \eta_j^A\}$ represent composite shadowing and fading in the interference channels and access channels, respectively. They follow identical Gamma-log-normal distributions with the PDF denoted as $f_{\xi\eta}(x)$. According to [18], $f_{\xi\eta}(x)$ can be approximated by a log-normal distribution as [18]

$$f_{\xi\eta}(x) \approx \frac{10}{\ln 10 \sqrt{2\pi}\sigma x} \exp\left\{-\frac{(10\log_{10} x - \mu)^2}{2\sigma^2}\right\}. \quad (17)$$

In (17), the mean μ and variance σ^2 are given by [18]

$$\mu = \epsilon^{-1}\left[\psi(m) - \ln(m)\right] \quad (18)$$

$$\sigma^2 = \epsilon^{-2}\zeta(2, m) + \sigma_\xi^2 \quad (19)$$

respectively, where $\epsilon = \ln(10)/10$ is a constant, $\psi(\cdot)$ is the Euler psi function, and $\zeta(\cdot,\cdot)$ is Riemann's zeta function [18]. When $m = 1$ this approximation is valid for $\sigma_\xi > 6$ dB, and for $m > 2$ the approximation is valid for all ranges of σ_ξ of interest [18]. The effect of Nakagami fading is to decrease the mean μ and increase the variance σ^2. Such an approximation allows us to use a single formula (17) to represent both pure-shadowing and composite shadowing and fading channels. When both shadowing and fading are in concern, we use (17) with μ in (18) and σ^2 in (19). In case only the shadowing is of interest, we can still use (17) with $\mu = 0$ and $\sigma^2 = \sigma_\xi^2$.

B. Transmit Power Distribution

Substituting (14) into (1) and (2), the CDF of the maximum allowable transmit power under realistic channels can be derived as (see Appendix)

$$F_{P_j^{\max}}(x) = 1 - \exp\left(-\lambda_p \pi Q (xK^I/I_0)^{2/\alpha}\right) \quad (20)$$

where

$$Q = \exp\left(\frac{2(\epsilon\mu\alpha + \epsilon^2\sigma^2)}{\alpha^2}\right). \quad (21)$$

Comparing (20) with (10), we can see that the transmit power CDFs under simple and realistic channel models only differ by a factor Q. This means that the transmit power CDF obtained under realistic channel models with a density parameter λ_p will be the same as the CDF obtained under simple channel models with a scaled density parameter $\lambda_p^* = \lambda_p Q$. In Table I, we show the values of Q under typical shadowing and fading scenarios. We can see that in most cases Q is close to 1, which indicates that such a scaling effect is not significant except for deep shadowing cases ($\sigma_\xi = 12$ dB). From (20), the corresponding PDF $f_{P_j^{\max}}(x)$ can be easily obtained as

$$f_{P_j^{\max}}(x) = \frac{2}{\alpha}\lambda_p \pi Q \left(\frac{K^I}{I_0}\right)^{\frac{2}{\alpha}} x^{\frac{2}{\alpha}-1} \exp\left(-\lambda_p \pi Q \left(x\frac{K^I}{I_0}\right)^{\frac{2}{\alpha}}\right). \quad (22)$$

C. Capacity Distribution

Using the transformation of random variables, the PDF of h_j^A can be derived from (15) as

$$f_{h_j^A}(x) = \frac{2(K^A)^{2/\alpha}}{\alpha R^2} Q x^{-1-2/\alpha} \Phi(g(x)) \quad (23)$$

where Q is given by (21), $\Phi(\cdot)$ is the CDF of a standard Gaussian distribution, and $g(x)$ is given by

$$g(x) = \frac{\ln(x) + \alpha\ln(R) - \ln(K^A) - \mu/\epsilon - \frac{2}{\alpha}(\epsilon\sigma)^2}{\epsilon\sigma}. \quad (24)$$

For convenience, we rewrite (3) in the dB form

$$(S_j)_{dB} = (P_j^{\max})_{dB} + (h_j^A)_{dB} \quad (25)$$

where $(S_j)_{dB} = 10\log_{10} S_j$, $(P_j^{\max})_{dB} = \log_{10} P_j^{\max}$, and $(h_j^A)_{dB} = 10\log_{10} h_j^A$. In (25), $(P_j^{\max})_{dB}$ is a random variable whose PDF can be derived from that of $P_j^{\max}$ as follows

$$f_{(P_j^{\max})_{dB}}(x) = \epsilon 10^{x/10} f_{P_j^{\max}}(10^{x/10}). \quad (26)$$

Similarly, the PDF of $(h_j^A)_{dB}$ is given by

$$f_{(h_j^A)_{dB}}(x) = \epsilon 10^{x/10} f_{h_j^A}(10^{x/10}). \quad (27)$$

Since $(P_j^{\max})_{dB}$ and $(h_j^A)_{dB}$ are mutually independent, the PDF of their sum $(S_j)_{dB}$ is the convolution of their individual PDFs, namely,

$$f_{(S_j)_{dB}}(x) = f_{(P_j^{\max})_{dB}}(x) * f_{(h_j^A)_{dB}}(x) \quad (28)$$

where "*" denotes convolution. The CDF $F_{(S_j)_{dB}}(x)$ of $(S_j)_{dB}$ can be obtained by taking the numerical integration of the PDF $f_{(S_j)_{dB}}(x)$. When opportunistic scheduling is considered, it follows that the CDF of $(S)_{dB} = 10\log_{10} S$ is given by

$$F_{(S)_{dB}}(x) = \left[F_{(S_j)_{dB}}(x)\right]^M . \quad (29)$$

Finally, the CDF of the capacity can be evaluated as

$$F_C(x) = F_{(S)_{dB}}\left(10\log_{10}\left(\Omega(2^x - 1)\right)\right). \quad (30)$$

V. Numerical Results and Discussions

Based on the above derived equations, the CDF $F_C(x)$ of the uplink capacity C will be evaluated numerically in this section. We focus on understanding the impacts of three key parameters on the distribution of C: the density of primary users λ_p, the cell radius R, and the number of opportunistically scheduled secondary users M. For other parameters that have direct scaling effects on the signal/interference strength, we take a simple treatment and normalize them to one, namely, we have $K^A = 1$, $K^I = 1$, $I_0 = 1$, and $\Omega = 1$. The pathloss exponent α is taken to be 4, which is a typical value in terrestrial cellular systems [18]. The default values of the three key parameters are taken as $\lambda_p = 0.001$ users/m^2, $R = 100$ m, and $M = 10$.

Moreover, we study the impacts of shadowing and fading on the capacity by comparing the capacity CDFs obtained with three types of channel models: the pathloss-only model, pathloss-shadowing model, and pathloss-shadowing-fading model. In Figs. 2 to 4, the capacity CDFs obtained with the pathloss-only and pathloss-shadowing channel models are compared to reveal the impacts of shadowing on the capacity. The shadowing standard deviation σ_ξ is taken as 8 dB. Furthermore, the impact of Nakagami fading on the capacity is studied in Fig. 5 by comparing the capacity CDFs obtained with pathloss-shadowing models to that with pathloss-shadowing-fading models.

Fig. 2 shows $F_C(x)$ with λ_p ranging from 0.001 to 0.01. For "pathloss-only" and "pathloss-shadowing" cases, $F_C(x)$ are calculated based on (13) and (30), respectively. The capacity is represented in the dB scale to cover the whole dynamic range. Clearly, the capacity is observed to have a reverse relationship with λ_p. This is expected since a denser population of primary receivers will impose tighter limits on the emission powers of the secondary transmitters. Since the channel capacity is a random variable, a particular useful measure of its statistical behavior is the so-called *outage* capacity. The β-outage capacity C_β is the capacity in (5) that can be surpassed with probability β: $P(C > C_\beta) = \beta$. From Fig. 2 we can see that such an outage capacity is sensitive to λ_p. For example, the difference between the 80%-outage capacities $C_{0.8}$ given by $\lambda_p = 0.001$ and $\lambda_p = 0.01$ is roughly 20 dB. This means that a ten times increase of the primary user density results in about one hundred times decrease in the 80%-outage capacity $C_{0.8}$. Moreover, from Fig. 2 we can see that the effect of shadowing on the capacity is to decrease the mean and increase the variance of the capacity distribution.

Similar to Fig. 2, Fig. 3 shows the impact of the secondary cell radius R on the capacity. Since the transmit powers of the secondary users are statistically limited by λ_p, one should choose a proper value for the cell radius R so that the BS is within a reasonable range to establish useful communication links. Despite the well-expected trend that the capacity decreases with increasing R, we observe that a 8 times increase of R (from 50 m to 400 m) results in roughly 1000 (30dB) times decrease in the 80%-outage capacity. Therefore, the outage capacity is even more sensitive to R than λ_p. Fig. 3 also shows similar impacts of shadowing on the capacity CDFs as that shown in Fig. 2.

Fig. 4 aims to show the benefits of opportunistic scheduling which exploits multi-user diversity. It is shown that a 20 dB gain on the 80%-outage capacity can be obtained by increasing the number of scheduled users from 2 to 20.

Finally in Fig. 5, we show the capacity CDFs with pathloss-shadowing-fading channel models. We change the value of the Nakagami shape factor m from 1 to 10000 to represent different fading scenarios. The case of $m = 1$ corresponds to Rayleigh fading, whereas $m = 10000$ approximates a pathloss-shadowing channel where there is no small scale fading. The results shows that small scale fading has trivial effects on the capacity distribution, with a $F_C(x)$ obtained from $m = 1$ virtually overlaps with that from $m = 10000$.

VI. Conclusions

In this paper, we have studied the uplink cell capacity of a cognitive radio network with a constraint on the peak interference power perceived by any primary receivers. We have considered a secondary cell of radius R to be deployed in a Poisson field of primary users whose density is given by λ_p. We have also assumed a secondary BS which opportunistically schedules among M secondary users to maximize the system capacity. The capacity has been studied as a random variable with both simple and realistic channel models. We have found that the capacity distribution reacts dramatically to smaller variations of parameters R, λ_p, and M. In addition, it has been shown that while shadowing can result in slight modifications on the capacity distribution, fading has neglectable impacts on the capacity. Our analysis provides a framework for future design and planning of similar cognitive radio networks.

Appendix
Derivation of (20)

The problem is to find the CDF of $P_j^{\max}$ defined in (2) where $h_j^{I_{\max}}$ and $h_{i,j}^I$ are given by (1) and (14), respectively. We will first work on the CDF $F_{h_j^{I_{\max}}}(x)$ of $h_j^{I_{\max}}$. Assume that a transmitting secondary user only interferes with primary receivers within a distance of L. Namely, the disk centered at the transmitting secondary user with a radius of L is considered as the effective interfering area. Given the primary receiver density λ_p, the probability that there are k primary receivers within the interfering disk area πL^2 is given by

$$f_k(k) = \frac{\exp\left(-\lambda_p \pi L^2\right)\left(\lambda_p \pi L^2\right)^k}{k!} \quad (k = 0, 1, \ldots, \infty). \tag{31}$$

Let $f_{h_j^{I_{\max}}}(x)$ denote the PDF of $h_j^{I_{\max}}$. Using the conditional probability we have

$$f_{h_j^{I_{\max}}}(x) = \sum_{k=0}^{\infty} f_k(k) f_{h_j^{I_{\max}}}(x|k) \tag{32}$$

where $f_{h_j^{I_{\max}}}(x|k)$ is the PDF of $h_j^{I_{\max}}$ conditioned on k. According to the property of Poisson point process, given that there are k primary users in the interfering disk, the location of these k primary users will follow independent and identical uniform distributions. Namely, $(d_{i,j}^I)^2$ in (14) have identical uniform distributions within $[0\ L^2]$. Since the composite shadowing and fading factor $\xi_{i,j}^I \eta_{i,j}^I$ are also independent and identically distributed, it follows that the distribution of $h_{i,j}^I$ are independent and identical. We use $f_{h_{i,j}^I}(x)$ and $F_{h_{i,j}^I}(x)$ to denote the PDF and CDF of $h_{i,j}^I$, respectively. The CDF of $h_j^{I_{\max}}$ conditioned on k is then given by

$$F_{h_j^{I_{\max}}}(x) = \left[F_{h_{i,j}^I}(x)\right]^k. \tag{33}$$

The differentiation of (33) gives the conditional PDF of $h_j^{I_{\max}}$

$$f_{h_j^{I_{\max}}}(x|k) = k\left[F_{h_{i,j}^I}(x)\right]^{k-1} f_{h_{i,j}^I}(x). \tag{34}$$

Substitute (34) into (32) and summing the exponential series we get

$$f_{h_j^{I_{\max}}}(x) = \lambda_p \pi L^2 f_{h_{i,j}^I}(x) \exp\left(-\lambda_p \pi L^2\left(1 - F_{h_{i,j}^I}(x)\right)\right). \tag{35}$$

Taking the indefinite integral of (35) will give the CDF of $h_j^{I_{\max}}$ as

$$F_{h_j^{I_{\max}}}(x) = \exp\left(-\lambda_p \pi L^2\left(1 - F_{h_{i,j}^I}(x)\right)\right). \tag{36}$$

Now we wish to obtain $F_{h_{i,j}^I}(x)$ in (36). It turns out that the deviations can be simplified if we involve another distribution function $F_{\left(h_{i,j}^I\right)^{-1}}(x)$: the CDF of $\left(h_{i,j}^I\right)^{-1}$. These two CDFs are related by

$$F_{h_{i,j}^I}(x) = 1 - F_{\left(h_{i,j}^I\right)^{-1}}\left(x^{-1}\right). \tag{37}$$

From (14) and (17), applying the transformation of random variables we have

$$F_{\left(h_{i,j}^I\right)^{-1}}(x) = \frac{2}{\alpha K^I L^2}\int_0^x F(z) z^{\frac{2}{\alpha}-1} dz \tag{38}$$

where

$$F(z) = \int_0^{L^\alpha/z} y^{\frac{2}{\alpha}} f_{\xi\eta}\left(\frac{y}{K^I}\right) dy. \tag{39}$$

Substituting (37), (38), and (39) into (36) and taking $L \to \infty$, after some mathematical manipulations we get

$$F_{h_j^{I_{\max}}}(x) = \exp\left(-\lambda_p \pi Q\left(\frac{K^I}{x}\right)^{\frac{2}{\alpha}}\right) \tag{40}$$

where Q is originally given by

$$Q = \int_0^{\infty} y^{\frac{2}{\alpha}} f_{\xi\eta}(y) dy \tag{41}$$

and can be further simplified to the form given in (21).

References

[1] Federal Communication Commission, Spectrum policy task force report, Washington DC, FCC 02-155, 2 Nov. 2002.
[2] Q. Zhao and B. M. Sadler, "A survey of dynamic spectrum access," IEEE Signal Processing Mag., vol. 24, no. 3, pp. 79–89, May 2007.
[3] S. Haykin, "Cognitive radio: brain-empowered wireless communications", *IEEE J. Selected Areas Commun.*, vol. 23, no. 2, pp. 201–220, Feb. 2005.
[4] I. F. Akyildiz, W. Y. Lee, M. C. Vuran and S. Mohanty, "NeXt generation/dynamic spectrum access/cognitive radio wireless networks: a survey", *Computer Networks*, vol. 50, no. 13, pp. 2127-2159, Sept. 2006.
[5] S. Srinivasa and S. A. Jafar, "The throughput potential of cognitive radio: a theoretical perspective," *IEEE Commun. Mag.*, vol. 45, no. 5, pp. 73–79, May 2007.
[6] M. Gastpar, "On capacity under receive and spatial spectrum-sharing constraints", *IEEE Trans. Inform. Theory*, vol. 53, no. 2, pp. 471–487, Feb. 2007.
[7] A. Ghasemi, and E. S. Sousa, "Capacity of fading channels under spectrum-sharing constraints," *Proc. IEEE ICC'06*, Istanbul, Turkey, June 2006, pp. 4373–4378.
[8] X. Hong, C.-X. Wang, and J. Thompson, "Uplink cell capacity of cognitive radio networks under interference outage constraints,", *Proc. IEEE ICCCAS'08*, Xiamen, China, May 2008, submitted.
[9] Federal Communication Commission, "Facilitating opportunities for flexible, efficient, and reliable spectrum use employing cognitive radio technologies", NPRM & Order, ET Docket No. 03-108, FCC 03-322, 30 Dec. 2003.
[10] T. Clancy. "Formalizing the interference temperature model," *Wiley J. Wireless Commun. and Mobile Computing*, vol. 7, no. 9, pp. 1077–1086, Nov. 2007.
[11] X. Hong, C.-X. Wang, and J. Thompson, "Interference modelling of cognitive radio networks in spectrum sharing systems", *Proc. IEEE VTC'08-Spring*, Singapore, May 2008, accepted.
[12] C.-X. Wang, H.-H. Chen, X. Hong, and M. Guizani, "Policy-based management for cognitive radio networks", *IEEE Veh. Techno. Mag.*, accepted.
[13] N. Devroye, P. Mitran, and V. Tarokh, "Achievable rates in cognitive radio channels," *IEEE Trans. Inform. Theory*, vol. 52, no. 5, pp. 1813–1827, May 2006.
[14] C.-X. Wang, X. Hong, H.-H. Chen, and J. S. Thompson, "On capacity of cognitive radio networks under average interference power constraints", *IEEE Trans. Wireless Commun.*, submitted.
[15] X. Hong, C.-X. Wang, H.-H. Chen, and J. Thompson, "On capacity of cognitive radio networks with average interference power constraints", *Proc. IEEE ICC'08*, Beijing, China, May 2008, accepted.
[16] S. Mangold, A. Jarosch, C. Monney, "Operator assisted cognitive radio and dynamic spectrum assignment with dual beacons – detailed evaluation," *Proc. First Int. Conf. Commun. Systems Software and Middleware*, Delhi, India, Jan. 2006, pp. 1–6.
[17] B. Wild and K. Ramchandran, "Detecting primary receivers for cognitive radio applications", *Proc. IEEE DySPAN'05*, Baltimore, USA, Nov. 2005, pp. 124-130.
[18] G. L. Stuber, *Principles of Mobile Communication*, 2nd Edition, Boston: Kluwer Academic Publishers, 2001.
[19] E. S. Sousa, "Performance of a spread spectrum packet radio network link in a poisson field of interferers," *IEEE Trans. Inform. Theory*, vol. 38, no. 6, pp. 1743-1754, Nov. 1992.
[20] A. Papoulis and S. U. Pillai, *Probability, Random Variables and Stochastic Processes*, 4th ed. New York: McGraw-Hill, 2002.

Table. I Vaules of Q given by (21) under different shadowing and fading scenarios ($\alpha = 4$)

	$m=1$	$m=2$	$m=4$	$m=16$	$m=\infty$
$\sigma_\xi = 6$ dB	1.0223	1.0518	1.7803	1.1022	1.1108
$\sigma_\xi = 8$ dB	1.1982	1.2328	1.2639	1.2919	1.3019
$\sigma_\xi = 10$ dB	1.7856	1.8371	1.8835	1.9252	1.9401
$\sigma_\xi = 12$ dB	4.8633	5.0036	5.1300	5.2435	5.2842

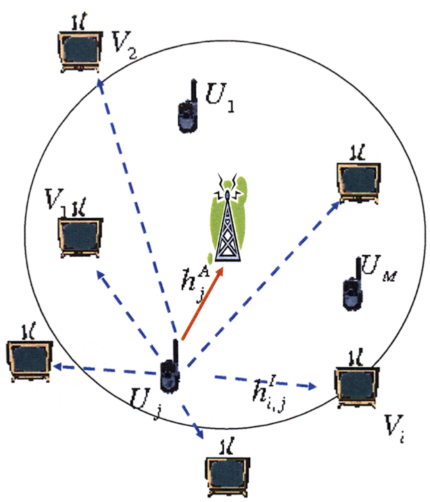

Fig. 1. System model.

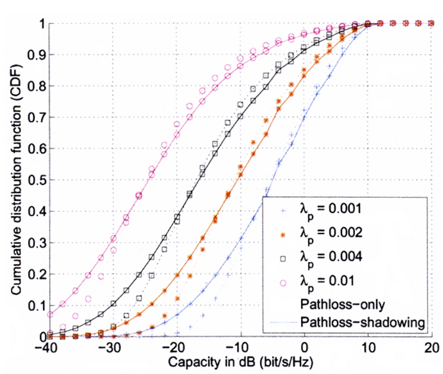

Fig. 2. CDFs of the capacity C with different values of λ_p, with and without shadowing ($K^A = 1$, $K^I = 1$, $I^0 = 1$, $\Omega = 1$, $R = 100$ m, $M = 10$, and $\sigma_\xi = 8$ dB).

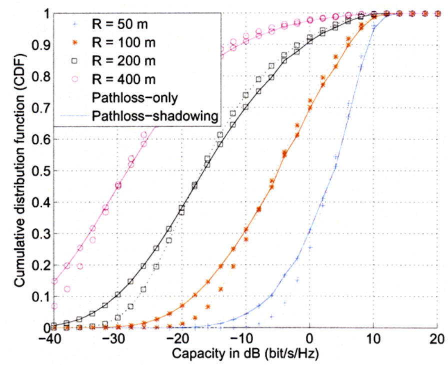

Fig. 3. CDFs of the capacity C with different values of R, with and without shadowing ($K^A = 1$, $K^I = 1$, $I^0 = 1$, $\Omega = 1$, $\lambda_p = 0.001$, $M = 10$, and $\sigma_\xi = 8$ dB).

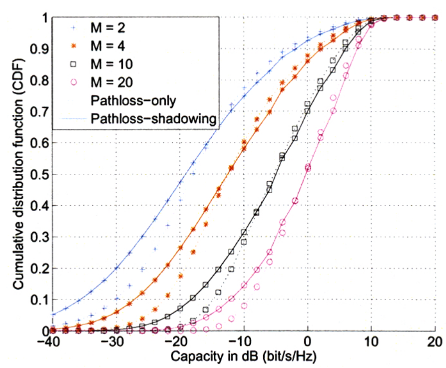

Fig. 4. CDFs of the capacity C with different values of M, with and without shadowing ($K^A = 1$, $K^I = 1$, $I^0 = 1$, $\Omega = 1$, $\lambda_p = 0.001$, $R = 100$ m, and $\sigma_\xi = 8$ dB).

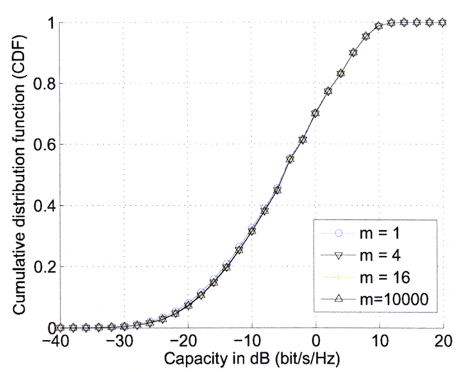

Fig. 5. CDFs of the capacity C with different values of Nakagami shaping factor m ($K^A = 1$, $K^I = 1$, $I^0 = 1$, $\Omega = 1$, $\lambda_p = 0.001$, $R = 100$ m, $M = 10$ and $\sigma_\xi = 8$ dB).